HHS Public Access

Author manuscript

Biochemistry. Author manuscript; available in PMC 2016 July 11.

Published in final edited form as:

Biochemistry. 2015 May 12; 54(18): 2851–2857. doi:10.1021/bi501540c.

Increased turnover under limiting [O_2] by the Thr^{387}→Ala variant of the HIF-prolyl hydroxylase PHD2

Serap Pektas[1], **Cornelius Y. Taabazuing**[1], and **Michael J. Knapp**[1,*]

[1]Department of Chemistry, University of Massachusetts, Amherst, MA 01003, United States

Abstract

PHD2 is a 2-oxoglutarate, non-heme Fe^{2+} dependent oxygenase that senses O_2 levels in human cells by hydroxylating two prolyl residues in the oxygen dependent degradation domain (ODD) of HIF1α. Identifying the active site contacts that determine the rate of reaction under limiting O_2 is crucial for understanding how these enzymes sense pO_2, and may suggest methods for chemically altering hypoxia responses. A hydrogen bonding network extends from the Fe(II) cofactor through ordered waters to the Thr^{387} residue in the second coordination sphere. Here we tested the impact of the sidechain of Thr^{387} on the reactivity of PHD2 toward O_2 through a combination of point mutagenesis, steady state kinetic experiments and {FeNO}^{7} EPR spectroscopy. The steady state kinetic parameters for Thr^{387}→Asn were very similar to those of WT-PHD2, but k_{cat} and $k_{cat}/K_{M(O2)}$ for Thr^{387}→Ala were increased by roughly 15-fold. X-band EPR spectroscopy of the {FeNO}^{7} centers of the (Fe+NO+2OG) enzyme forms showed the presence of a more rhombic line shape in Thr^{387}→Ala than seen for WT-PHD2, indicating an altered conformation for bound gas in this variant. Here we show that the sidechain of residue Thr^{387} plays a significant role in determining the rate of turnover by PHD2 at low [O_2].

Graphical abstract

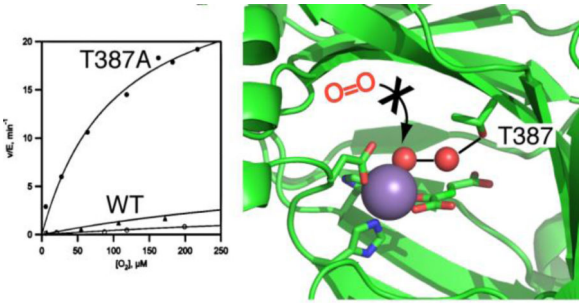

Keywords

HIF; hypoxia; non-heme iron; 2-oxoglutarate; HIF-prolyl hydroxylase

mknapp@chem.umass.edu, Voice: (413) 545-4001, Fax: (413) 545-4490.

The authors declare no competing financial interest.

Supporting Information

Experimental measurement of $K_{D(2OG)}$ for PHD2 variants. The material is available free of charge via the Internet at http://pubs.acs.org.

Introduction

HIF prolyl-4-hydroxylase 2 (PHD2) is a non heme Fe(II), 2-oxoglutarate (2OG) dependent oxygenase that serves as the primary O_2 sensor in human cells[1,2]. PHD2 regulates the transcriptional activity of the hypoxia-inducible factor-1α (HIF-1α) transcription factor by hydroxylating Pro^{402} and Pro^{564} within the oxygen dependent degradation domain (ODD) of HIF-1α[1,3–5]. As HIF-1α hydroxylation underlies angiogenesis and the balance between aerobic/anaerobic metabolism, PHD2 plays a crucial role in health conditions such as ischemia, anemia, and cancer[6,7]. Identifying the structural features of PHD2 that determine the reaction rate under conditions of limiting [O_2] could point the way to altering cellular hypoxia sensing.

The (Fe+2OG)PHD2 form of enzyme contains an Fe(II) cofactor coordinated by a His_2Asp facial triad, a bidentate 2OG ligand, and an aquo ligand. PHD2 is thought to follow the consensus chemical mechanism for 2OG oxygenases (Scheme 1).[8–10] When substrate ODD binds near the cofactor, the aquo ligand is released in analogy to other 2OG oxygenases, permitting O_2 to bind at the Fe for subsequent chemistry. Oxidative decarboxylation generates the ferryl $(FeO)^{2+}$, an intermediate that has been observed in related enzymes,[8,9,11,12] which hydroxylates the Pro target residue to complete the chemical steps of turnover (Scheme 1). Notably, PHD2 appears to be rate-limited by a step associated with O_2 binding or oxidative decarboxylation, as the $(FeO)^{2+}$ intermediate did not accumulate in the pre-steady state for PHD2,[10] and PHD2 exhibited an inverse solvent kinetic isotope effect (KSIE).[13,14] This is in contrast to other 2OG oxygenases that accumulate the $(FeO)^{2+}$ in the pre-steady state, for which product release or hydroxylation appear to be rate-limiting step.[8,9,11,12]

The connection between substrate binding and O_2 activation is crucial to understanding the chemistry of this class of enzyme. A recent study revealed a conserved pattern of second-sphere contacts in enzymes structurally related to PHD2[15] which may be functionally significant. The X-ray crystal structure of (Fe+2OG)PHD2[16] showed a hydrogen bonding network connecting the aquo ligand and 2OG to the sidechain of Thr^{387} (Figure 1). Thr^{387} is located on the second β strand, at a position which forms a conserved H-bond in many 2OG oxygenases.[15] As O_2 activation is integral to the function of PHD2 and other 2OG oxygenases, the disposition of Thr^{387} may be crucial to gas binding and reactivity.

Here we tested the role of second sphere contacts from Thr^{387} on PHD2 hydroxylation chemistry through steady state kinetics and $\{FeNO\}^7$ EPR spectroscopy. Steady-state kinetic parameters for the $Thr^{387}\rightarrow$Asn variant, which conserved the hydrogen bonding capacity at this position, were very similar to those of WT-PHD2. Remarkably, the macroscopic rate constants for the $Thr^{387}\rightarrow$Ala variant were 15 times larger than for WT-PHD2, which is attributed to faster O_2 activation. Substrate inhibition was observed for the $Thr^{387}\rightarrow$Ala variant, which implicates product release as a slow step in this variant – a corollary is that other substrate inhibition in other 2OG oxygenases likely reflects slow succinate release[17]. These results suggest that the second sphere contacts from Thr^{387} slow turnover such that decarboxylation chemistry is rate-limiting in WT-PHD2.

Materials and Methods

Materials

All chemicals were purchased from commercial vendors, and used without purification. The sequences of the peptide substrates were derived from the native HIF-1α$^{556–574}$ (CODD) sequence. The sequence of the CODD peptide was DLDLEALA**P**^{564}YIPADDDFQL. The underlined residues were changed from the native sequences as follows: CODD (M561A, M568A) to avoid methionine oxidation. The CODD peptide (99 % purity) was purchased from GL Biochem LTD (Shanghai).

Protein expression and purification

Recombinant human PHD2$_{178–426}$ and its variants, Thr^{387}→Ala and Thr^{387}→Asn were expressed as a C-terminal GST fusion protein from *E. coli* BL21(DE3) cells using a pGEX-4T-1 vector (Stratagene) and purified as previously described[14,18]. Briefly, PHD2-GST was purified using an affinity column (GSTrap, GE Bioscience), then the GST-tag was cleaved with restriction grade thrombin for 16 hours at 4 °C. The thrombin was removed with a Hitrap Benzamidine column (GE Bioscience), then PHD2 was treated with 50 mM EDTA overnight to remove metals. PHD2 was buffer exchanged with 50 mM HEPES pH 7.50 and stored at −20 °C. The mass of the WT-PHD2 and the variants were determined by a QStar-XL hybrid quadrupole-TOF mass spectrometer (Applied Biosystems). WT-PHD2 (27786.6 Da calculated, 27784.7 Da observed), Thr^{387}→Ala (27755.2 Da calculated, 27756.2 Da observed), and Thr^{387}→Asn (27799.6 Da calculated, 27798.2 Da observed).

Steady state kinetic assays

Steady-state kinetic constants were obtained from initial rates were measured under saturating concentrations of $(NH_4)_2Fe(SO_4)_2$ (10 μM) and ascorbic acid (1 mM) in 50 mM HEPES buffer pH 7.00 at 37.0 °C. MALDI-TOF was used to measure the production of of hydroxylated product CODD^{OH} ((M+O+Na$^+$): 2174 m/z calc., 2172 m/z obs.) from the substrate peptide CODD ((M+Na$^+$): 2158 m/z calc., 2156 m/z obs.). Substrate inhibition constants were obtained by fitting the initial-rate data to Eq. 1, in which the initial rate (v_o) is a function of the maximal rate (v_{max}), the Michaelis constant (K_M) and the inhibition constant (K_i) for the substrate (S).

$$v_0 = \frac{V_{max}}{1 + \frac{K_M}{[S]} + \frac{[S]}{K_i}} \quad \text{(Equation 1)}$$

For assays in which [2OG] was varied, the concentration of CODD (10 μM) was fixed at saturating levels. Reactions were quenched at different time points in saturated 4-α-cyano hydroxycinnamic acid dissolved in 75 % acetonitrile and 0.2 % trifluoroacetic acid. Quenched reactions were spotted onto a MALDI target plate and analyzed using a Bruker Daltonics Omniflex MALDI-TOF mass spectrometer. For assays in which the [CODD] varied, the concentration of 2OG (100 μM) was fixed at saturating.

Assays in which O_2 was the varied substrate used saturating concentrations of $(NH_4)_2Fe(SO_4)_2$ (10 μM), 2OG (100 μM), CODD (10 μM) and ascorbic acid (1 mM) in 50 mM HEPES pH 7.00 at 37 °C. The concentration of dissolved O_2 was controlled by varying the ratio of N_2 and O_2 gas flowing through separate flow meters through a gas washer into an Atmosbag (Sigma-Aldrich), with the dissolved O_2 concentration monitored by a YSI model 5300 biological oxygen monitor. Reactions were quenched and analyzed as for other steady state reactions.

2OG Binding

The dissociation constant (K_D) of 2OG was determined by measuring the quenching of the intrinsic tryptophan fluorescence of PHD2 upon binding 2OG. Samples were excited at 295 nm and the emission measured at 330 nm using a PTI spectrofluorometer (PTI-QM-4 2005SE). A cuvette containing PHD2 (1 μM), and $MnSO_4$ (20 μM) in 50 mM HEPES pH 7.00 was titrated with aliquots of 2OG (500 μM); the K_D was obtained by fitting the data to equation 2, in which the observed fluorescence intensity (I) is normalized to the intensity in the absence of 2OG (I_0) and the presence of saturating [2OG] (I_f).

$$\frac{I - I_0}{I_f - I_0} = \frac{([PHD2]+[2OG]+K_D) - \sqrt{([PHD2]+[2OG]+K_D)^2 - (4[PHD2][2OG])}}{2[PHD2]}$$

(Equation 2)

X-band EPR of {FeNO}^{7}

Anaerobic samples were prepared a glovebox ($[O_2]$ < 1 ppm) for analysis. $(NH_4)_2FeSO_4$ was brought into the glovebox as a solid and dissolved using degassed H_2O. The DEANO stocks were prepared in 10 mM NaOH in the glovebox and the concentration verified by its published extinction coefficient and characteristic UV absorbance at 250 nm.[19,20] A 100 μL EPR sample was prepared anaerobically and contained PHD2 (0.10 mM), $(NH_4)_2FeSO_4$, (0.10 mM), 2OG (0.50mM), CODD (100 μM) and DEANO (0.5 mM) in 50 mM HEPES pH 7.00 at room temperature (23°C). The sample was aged for 20 minutes to allow NO release from DEANO, then flash frozen in liquid nitrogen. EPR spectra were collected using a Bruker Elexsys E-500 EPR equipped with a DM4116 cavity and a Bruker ER 4118CF-O LHe/LN_2 cryostat at 9.624 GHz frequency, 2.0 mW power, 10 G modulation amplitude, 100 GHz modulation frequency, 163 ms time constant, 4 K. As the electronic structure of the S = 3/2 ferrous-nitrosyl center is highly axial (E/D < 0.1), the observed EPR resonances ($g_{x,y,z}$) were related to the rhombicity of the zero field splitting (E/D) using an effective spin Hamiltonian (Eq. 3).[21]

$$g_x = g_0\left[2 - 3E/D - 3/2\,(E/D)^2\right] \quad \text{(Eq. 3a)}$$

$$g_y = g_0 \left[2 + {}^{3E}/_{D} - {}^{3}/_{2} \left({}^{E}/_{D} \right)^2 \right] \quad \text{(Eq. 3b)}$$

$$g_z = g_0 \left[1 - 3 \left({}^{E}/_{D} \right)^2 \right] \quad \text{(Eq. 3c)}$$

Results and Discussion

Steady state kinetics with varied [2OG]

The structure of PHD2 showed a hydrogen bond network connecting 2OG, the aquo ligand, and Thr^{387} (Figure 1). As a hydrogen bonding residue is structurally conserved at this position in other 2OG oxygenases,[13,15] we hypothesized that this played an important role during turnover. To test the effect of this contact on steps between 2OG binding and ODD binding, initial rate data were measured as a function of varied [2OG] using saturating concentrations of Fe^{2+} (10 μM), CODD (10 μM), and ascorbate (1 mM); [O_2] was fixed at ambient levels (217 uM). WT-PHD2 exhibited simple saturation kinetics over the range of 1 – 50 μM 2OG, with values of k_{cat} (2.3 min^{-1}) and $k_{cat}/K_{M(2OG)}$ (2.7 $\mu M^{-1} min^{-1}$) similar to those previously reported[14,18,22–24]. Similarly, the conservative Thr^{387}→Asn variant exhibited saturation kinetics over the tested concentration range, with modestly decreased rate constants relative to WT-PHD2 (Table 1).

The initial rate data for the Thr^{387}→Ala variant was a significant contrast to that of WT-PHD2. While Thr^{387}→Ala exhibited simple saturation kinetics for [2OG] < 250 μM, this variant exhibited ~50% activity at 3000 μM 2OG (Figure 2). Fitting the initial rate data to a simple substrate inhibition model led to parameters of k_{cat} (32.9 min^{-1}), $k_{cat}/K_{M(2OG)}$ (2.7 $\mu M^{-1} min^{-1}$), and $K_{I(2OG)}$ (2200 μM). The high value for k_{cat} indicated that Thr^{387}→Ala performed chemistry more rapidly than WT-PHD2, but the observed substrate inhibition suggested that slow release of one of the products could limit turnover.

The steady state rate constant $k_{cat}/K_{M(2OG)}$ reflects those steps between 2OG binding and the subsequent irreversible step, which is CODD binding under conditions of saturating [CODD]. As this rate constant is essentially unchanged upon mutation of Thr^{387}, contacts from this residue do not affect these steps. In contrast, k_{cat} reflects non-diffusional steps, and was greatly affected by mutation of Thr^{387}. While k_{cat} was unchanged in the conservative Thr^{387}→Asn variant, this kinetic parameter increased ~ 15 fold for the Thr^{387}→Ala variant, suggesting that a chemical step was affected by the Thr^{387} variants.

The substrate inhibition observed for Thr^{387}→Ala prompted us to test the other variants for this effect. WT-PHD2 retained >95% activity even at extremely high levels of 2OG; fits of this data to the substrate inhibition model were unsatisfactory ($K_{I(2OG)}$ >26 mM) indicating that PHD2 did not undergo substrate inhibition. Thr^{387}→Asn similarly showed minimal inhibition at extremely high 2OG concentration ($K_{I(2OG)}$ >50 mM). The absence of significant substrate inhibition observed for WT-PHD2 was consistent with product release

being rapid, consistent with the prior reports that implicated a step early in catalysis as being rate-limiting for WT-PHD2[10].

Substrate inhibition could arise from many possible mechanisms in which substrate binding leads to an enzyme form of lower reactivity. Inhibition by 2OG could be due to 2OG binding to the Fe^{2+} cofactor in a geometry that prevented O_2 from reacting, or by binding to the Fe^{2+} when an equivalent of succinate or 2OG was already present. Although our kinetics data and 2OG binding data cannot distinguish among these possibilities, a unified model that accounts for the observed kinetics (see below) and substrate inhibition found for Thr^{387}→Ala is one in which chemistry is much faster than succinate release, such that the (Fe+Succ)PHD2 form of enzyme accumulates in the steady state for this variant. Inhibition by 2OG or by CODD would arise from these substrates binding to the (Fe+Succ)PHD2 form of enzyme, thereby preventing the enzyme from adopting the proper cofactor orientation to enter into catalysis.

The binding affinity for 2OG was measured for each of the variants by intrinsic tryptophan fluorescence quenching (supplemental material). Binding curves were fit to a single binding site model using Eq. 2, which indicated a similar avidity toward 2OG (K_D ~ 1 μM) for each variant. Attempts to fit a second 2OG binding event were not successful, possibly due to the large difference in magnitude between $K_{M(2OG)}$ and $K_{I(2OG)}$ for each of the variants.

Steady state kinetics with varied [CODD]

The impact of Thr^{387} variants on the chemical steps of turnover was tested by measuring steady state kinetics with CODD as the varied substrate. Initial rates of CODD hydroxylation were measured as a function of varied CODD concentration in 50 mM HEPES (pH 7.00, 37.0 °C), with saturating concentrations of Fe^{2+} (10 μM), 2OG (100 μM), and ascorbate (1 mM); the [O_2] was fixed at the ambient level (217 μM). As O_2 was not saturating, $k_{cat}/K_{M(CODD)}$ will reflect steps spanning CODD binding up through the irreversible chemistry involved with oxidative decarboxylation. Steady state kinetic constants, k_{cat}, and $k_{cat}/K_{M(CODD)}$, were determined by fitting the data to the Michaelis-Menten equation (Figure 3). The rate constants for WT-PHD2 were in good agreement with prior reports[14,22,25]. While the conservative Thr^{387}→Asn mutation led to rate constants that were modestly decreased from those of WT-PHD2, those for the Thr^{387}→Ala variant were ~ 10 fold *greater* than those of WT-PHD2, indicating that removal of the hydrogen bond from Thr^{387} greatly impacted chemical steps. The rate constants for the Thr^{387}→Ala also exhibited pronounced substrate inhibition at elevated CODD concentrations (Figure 3).

The initial rate data for Thr^{387}→Ala was fit in two ways in order to adequately treat the inhibition. The first fit used the Michaelis-Menten equation to fit the initial rate data for [CODD] < 10 μM, leading to fitted parameters of k_{cat} = 33 min^{-1} and $k_{cat}/K_{M(CODD)}$ = 13 $\mu M^{-1}min^{-1}$. These kinetic constants were remarkable because they suggested that the active site in WT-PHD2 was arranged to slow turnover.

The second fit used the substrate inhibition model and resulted in k_{cat} = 44 min^{-1}, $k_{cat}/K_{M(CODD)}$ = 11 $\mu M^{-1}min^{-1}$, and K_I = 38 μM (Table 2). This second fit reproduced the data well, suggesting that the peptide substrate (CODD) was a stronger inhibitor than 2OG

toward the Thr^{387}→Ala variant. As for 2OG inhibition, inhibition by the CODD substrate could arise from many possible mechanisms in which CODD binding would lead to a low-activity enzyme form. A simple model that accounts for the kinetic changes for the Thr^{387}→Ala variant is one in which succinate release is slow, as this could lead to either 2OG or CODD binding to the unreactive (Fe+succ)PHD2 enzyme form. The substrate inhibition by 2OG and CODD implicate a step after O_2 binding/activation as rate-limiting in the Thr^{387}→Ala variant.

Steady state kinetics with varied [O_2]

The increased rates of turnover for the Thr^{387}→Ala variant suggested that steps involved in O_2 activation were faster than for WT-PHD2. The steady-state kinetics as a function of varied O_2 concentration were measured to isolate steps between O_2 binding and oxidative decarboxylation. The initial rate data showed simple saturation kinetics for all but the Thr^{387}→Ala variant, and was fit to the Michaelis-Menten equation (Figure 4). Both WT-PHD2 and the conservative Thr^{387}→Asn variant exhibited sluggish reactivity toward O_2, with the kinetic parameters for WT-PHD2 $k_{cat}/K_{M(O2)}$ = 0.015 μM^{-1}min-1 (~ 0.25 × 10^{-9} M^{-1} sec^{-1}) and $K_{M(O2)}$ = 530 μM consistent with prior reports[28,29]. The high $K_{M(O2)}$ has been rationalized as being necessary for hypoxia sensing, as PHD2 activity would be proportionate to physiologically relevant levels of [O_2].[30] The Thr^{387}→Ala variant is a contrast to this, as $k_{cat}/K_{M(O2)}$ = 0.3 μM^{-1} min^{-1}, a 20-fold increase in reaction rate over that of WT-PHD2 which indicates that step(s) involving O_2 activation have markedly increased in rate for this variant. The Thr^{387}→Ala variant also exhibited saturation kinetics up to 220 μM O_2, but with an activity that was only ~25% of maximal at elevated O_2 concentrations (Fig. 4). Attempts at fitting this activity curve to a variety of inhibition models led to unsatisfactory fits, suggesting that the decreased activity at high [O_2] may reflect enzyme inactivation, as is seen for several other 2OG oxygenases.[31–34]

As our experimental conditions used saturating levels of 2OG and CODD, the macroscopic rate constant ($k_{cat}/K_{M(O2)}$) reports only on steps between O_2 binding and the subsequent irreversible step, which in the consensus mechanism for PHD2 is oxidative decarboxylation. The increased values for k_{cat} and $k_{cat}/K_{M(O2)}$ observed for Thr^{387}→Ala point definitively to an increased rate for oxidative decarboxylation in this variant over that observed for WT-PHD2.

The kinetic parameters for the Thr^{387}→Ala variant are remarkable for two reasons. First, the increased $k_{cat}/K_{M(O2)}$ and related mechanistic data indicate that chemistry has become faster as a result of this point mutation, underscoring the enormous influence over oxidative decarboxylation exerted by 2°-sphere contacts in PHD2. This implies that O_2-activation is not just a function of the redox potential at the Fe^{2+} cofactor, but will include the polar environment near the 2OG and the distal O-atom of bound O_2. Second, the Thr^{387}→Ala variant has a lower $K_{M(O2)}$ than found for WT-PHD2, making for a more sensitive activity response to changes in [O_2], particularly over the physiological range of [O_2] < 50 μM. This opens the possibility of using enzyme delivery[35] or engineering approaches to tailor the hypoxia response within cells.

EPR spectra of ($Fe^{2+}NO$) PHD2

According to the consensus mechanism, PHD2 must bind O_2 such that the distal O-atom can attack the 2-oxo position of 2OG. We propose that the Thr^{387} of WT-PHD2 favors a specific gas binding geometry such that the bound O_2 is not positioned optimally for reaction with 2OG. As NO binds to Fe^{2+} in non-heme enzymes to form a spectroscopically accessible $\{FeNO\}^7$ with S = 3/2, and adopts a bent geometry similar to that of bound O_2[27,36,37],) we used EPR lineshape analysis to assess the impact of Thr^{387} on bound gas geometry.

The EPR lineshape of $\{FeNO\}^7$ centers in 2OG oxygenases and related enzymes is dominated by the large zero-field splitting,[36–38] with EPR features near g_{eff} ~ 2 and g_{eff} ~ 4 that are sensitive reporters of the rhombic zero-field splitting parameter (E/D).[21] Rhombic zero-field splitting can be directly calculated by use of Eq. 3, relating the observed g_{eff} values to the E/D ratio. As the zero-field splitting arises from admixture of the low-lying excited states into the ground state, the E/D ratio ultimately reports on the geometry of the $\{FeNO\}^7$ spin center. For example, the EPR lineshape of the $\{FeNO\}^7$ center is very sensitive to the Fe-NO bond angle in sterically constrained models complexes[39] as well as equatorial bonding in non-heme proteins[21,37] due to the splitting of the g_{eff} ~ 4 features caused by rhombic zero-field splitting.

Ferrous nitrosyl complexes of WT-PHD2 and the $Thr^{387}\rightarrow$Ala variant were prepared by anaerobically generating NO in the presence of the (Fe+2OG)PHD2/CODD form of each enzyme. The X-band EPR spectra were collected at 4 K in a liquid helium flow cryostat, showing a complex lineshape near g_{eff} = 4 for both samples (Figure 5). The $\{FeNO\}^7$ center of WT-PHD2 exhibited intense features at g_{eff} = 4.08, 3.96, which arose from an S=3/2 spin with a highly axial zero-field splitting (E/D = 0.011); as well as a minor feature at g_{eff} ~ 4.3 that likely arose from adventitious Fe^{3+}. In contrast, the $\{FeNO\}^7$ center of $Thr^{387}\rightarrow$Ala was more complex, with two S = 3/2 species evident. One species was very similar to that observed for WT-PHD2, with g_{eff} = 4.09, 3.94 (E/D = 0.014); the second center was much more rhombic, g_{eff} = 4.33, 3.75 (E/D = 0.48).

Although it is not possible to ascribe specific geometries to each of these spin centers, the $Thr^{387}\rightarrow$Ala mutation lead to a much more heterogeneous $\{FeNO\}^7$ center than found in WT-PHD2. This likely arose from the steric interactions between the bound NO and contacts with the active site environment. Coupled with the observed increase in activity for $Thr^{387}\rightarrow$Ala, this suggests that the geometry of bound gas is correlated with O_2 activation such that WT-PHD2 positions the bound gas in a non-optimal orientation for oxidative decarboxylation. In the consensus mechanism O_2 binds as a putative (Fe^{3+} $O_2^{—}$) adduct, which then attacks the C-2 keto position of 2OG to initiate oxidative decarboxylation. Should the distal O-atom be stabilized by an electric dipole interaction with the hydroxyl group of Thr^{387}, it could be less nucleophilic in WT-PHD2. Alternately, Thr^{387} could cause the distal O-atom to be oriented away from the C-2 keto position, thereby lowering the reactivity of the putative superoxide in WT-PHD2.

Implications for hypoxia sensing

Why is turnover so slow for WT-PHD2, and how could removing the hydrogen bonds from Thr^{387} increase the kinetic parameters for O_2 activation? The answers to both of these questions are speculative at this point, but considering the structural and mechanistic data for PHD2 within the context of the physiological role of this enzyme points to the intriguing possibility that the naturally occurring residue is part of the machinery that limits maximal turnover.

As the physiological role of PHD2 is to turn off gene expression, it is very likely that this enzyme fulfills its role while turning over on the minutes timescale – this lack of evolutionary pressure to increase reaction rates may lead to an active site optimized for something other than rapid turnover. Single turnover experiments indicated that hydroxylated CODD product formed on the minutes timescale (k_{obs} = 0.018 s^{-1}, 5°C) without any accumulating intermediates.[10] As this rate constant is virtually identical to that observed in the steady state (k_{cat} = 0.03 s^{-1}, 37 °C)[14], it is very likely that oxidative decarboxylation is rate-limiting in WT-PHD2. This is unusual for 2OG-dependent oxygenases, but may reflect the O_2-sensing from the function of PHD2.

The implication of this work are two-fold. First, contacts within the active site control the O_2 activation rate in 2OG oxygenases. Second, PHD2 can be engineered into a more active form than found in nature, in particular with respect to the reactivity under low [O_2] conditions. Although this was achieved by point mutagenesis in the current report, one can envision the use of small molecules to target the distal hydrogen-bonding in PHD2. Achieving increased turnover under hypoxic conditions would lead to altered cellular hypoxia sensing.

Supplementary Material

Refer to Web version on PubMed Central for supplementary material.

Acknowledgments

Funding This research was supported by the U.S. National Institutes of Health (1R01-GM077413 to M.J.K), the NIH Chemistry-Biology Interface Predoctoral Training Grant (T32-GM008515 to C. Y. T.) and the Turkish Ministry of National Education (S.P.).

Abbreviations

2OG	2-oxo-glutarate, α-ketoglutarate
AtsK	Alkylsulfatase
FIH	factor-inhibiting HIF
HAT	hydrogen atom transfer
HEPES	4-(2-hydroxyethyl)-1-piperazineethanesulfonic acid
HIF	hypoxia inducible factor-1α

MALDI-TOF-MS	Matrix assisted laser desorption ionization-time of flight-mass spectrometry
PHD2	prolyl hydroxylase domain 2
TauD	taurine dioxygenase

Bibliography

1. Berra E, Benizri E, Ginouvès A, Volmat V, Roux D, Pouysségur J. HIF prolyl-hydroxylase 2 is the key oxygen sensor setting low steady-state levels of HIF-1alpha in normoxia. EMBO J. 2003; 22:4082–4090. [PubMed: 12912907]
2. Appelhoff RJ, Tian Y-M, Raval RR, Turley H, Harris AL, Pugh CW, Ratcliffe PJ, Gleadle JM. Differential function of the prolyl hydroxylases PHD1, PHD2, and PHD3 in the regulation of hypoxia-inducible factor. J. Biol. Chem. 2004; 279:38458–38465. [PubMed: 15247232]
3. Bruick RK. Oxygen sensing in the hypoxic response pathway: regulation of the hypoxia-inducible transcription factor. Genes Dev. 2003; 17:2614–2623. [PubMed: 14597660]
4. Jaakkola P, Mole DR, Tian YM, Wilson MI, Gielbert J, Gaskell SJ, Kriegsheim Av, Hebestreit HF, Mukherji M, Schofield CJ, Maxwell PH, Pugh CW, Ratcliffe PJ. Targeting of HIF-alpha to the von Hippel-Lindau ubiquitylation complex by O2-regulated prolyl hydroxylation. Science. 2001; 292:468–472. [PubMed: 11292861]
5. Aprelikova O, Chandramouli GVR, Wood M, Vasselli JR, Riss J, Maranchie JK, Linehan WM, Barrett JC. Regulation of HIF prolyl hydroxylases by hypoxia-inducible factors. J. Cell. Biochem. 2004; 92:491–501. [PubMed: 15156561]
6. Hewitson KS, Schofield CJ. The HIF pathway as a therapeutic target. Drug Discov. Today. 2004; 9:704–711. [PubMed: 15341784]
7. Speer RE, Karuppagounder SS, Basso M, Sleiman SF, Kumar A, Brand D, Smirnova N, Gazaryan I, Khim SJ, Ratan RR. Hypoxia-inducible factor prolyl hydroxylases as targets for neuroprotection by “antioxidant” metal chelators: From ferroptosis to stroke. Free Radic. Biol. Med. 2013; 62:26–36. [PubMed: 23376032]
8. Hoffart LM, Barr EW, Guyer RB, Bollinger JM, Krebs C. Direct spectroscopic detection of a C-H-cleaving high-spin Fe(IV) complex in a prolyl-4-hydroxylase. Proc. Natl. Acad. Sci. U. S. A. 2006; 103:14738–14743. [PubMed: 17003127]
9. Krebs C, Galonić Fujimori D, Walsh CT, Bollinger JM. Non-heme Fe(IV)-oxo intermediates. Acc. Chem. Res. 2007; 40:484–492. [PubMed: 17542550]
10. Flashman E, Hoffart LM, Hamed RB, Bollinger JM, Krebs C, Schofield CJ. Evidence for the slow reaction of hypoxia-inducible factor prolyl hydroxylase 2 with oxygen. FEBS J. 2010; 277:4089–4099. [PubMed: 20840591]
11. Price JC, Barr EW, Tirupati B, Bollinger JM, Krebs C. The first direct characterization of a high-valent iron intermediate in the reaction of an alpha-ketoglutarate-dependent dioxygenase: a high-spin FeIV complex in taurine/alpha-ketoglutarate dioxygenase (TauD) from Escherichia coli. Biochemistry. 2003; 42:7497–7508. [PubMed: 12809506]
12. Grzyska PK, Ryle MJ, Monterosso GR, Liu J, Ballou DP, Hausinger RP. Steady-state and transient kinetic analyses of taurine/alpha-ketoglutarate dioxygenase: effects of oxygen concentration, alternative sulfonates, and active-site variants on the FeIV-oxo intermediate. Biochemistry. 2005; 44:3845–3855. [PubMed: 15751960]
13. Hangasky JA, Saban E, Knapp MJ. Inverse Solvent Isotope Effects Arising from Substrate Triggering in the Factor Inhibiting Hypoxia Inducible Factor. Biochemistry. 2013; 52:1594–1602. [PubMed: 23351038]
14. Flagg SC, Giri N, Pektas S, Maroney MJ, Knapp MJ. Inverse solvent isotope effects demonstrate slow aquo release from hypoxia inducible factor-prolyl hydroxylase (PHD2). Biochemistry. 2012; 51:6654–6666. [PubMed: 22747465]

15. Hangasky, Ja; Taabazuing, CY.; Valliere, Ma; Knapp, MJ. Imposing function down a (cupin)-barrel: secondary structure and metal stereochemistry in the αKG-dependent oxygenases. Metallomics. 2013; 5:287–301. [PubMed: 23446356]

16. Rosen MD, Venkatesan H, Peltier HM, Bembenek SD, Kanelakis KC, Zhao LX, Leonard BE, Hocutt FM, Wu X, Palomino HL, Brondstetter TI, Haugh PV, Cagnon L, Yan W, Liotta La, Young A, Mirzadegan T, Shankley NP, Barrett TD, Rabinowitz MH. Benzimidazole-2-pyrazole HIF Prolyl 4-Hydroxylase Inhibitors as Oral Erythropoietin Secretagogues. ACS Med. Chem. Lett. 2010; 1:526–529. [PubMed: 24900242]

17. Cascella B, Mirica LM. Kinetic analysis of iron-dependent histone demethylases: α-ketoglutarate substrate inhibition and potential relevance to the regulation of histone demethylation in cancer cells. Biochemistry. 2012; 51:8699–8701. [PubMed: 23067339]

18. Pektas S, Knapp MJ. Substrate preference of the HIF-prolyl hydroxylase-2 (PHD2) and substrate-induced conformational change. J. Inorg. Biochem. 2013; 126:55–60. [PubMed: 23787140]

19. Maragos CM, Morley D, Wink DA, Dunams TM, Saavedra JE, Hoffman A, Bove AA, Isaac L, Hrabie JA, Keefer LK. Complexes of NO with Nucleophiles as Agents for the Controlled Biological Release of Nitric Oxide. Vasorelaxant Effects. J. Med. Chem. 1991; 34:3242–3247. [PubMed: 1956043]

20. Keefer LK, Nims RW, Davies KM, Wink DA. “NONOates” (1-Substituted Diazen-1-ium-1,2-diolates) as Nitric Oxide Donors: Convenient Nitric Oxide Dosage Forms. Methods Enzymol. 1996; 268:281–293. [PubMed: 8782594]

21. Arcierog DM, Orville AM, Lipscomb JD. [l ‘ O] Water and Nitric Oxide Binding by Protocatechuate. J. Biol. Chem. 1985; 260:14035–14044. [PubMed: 2997190]

22. Flagg SC, Martin CB, Taabazuing CY, Holmes BE, Knapp MJ. Screening chelating inhibitors of HIF-prolyl hydroxylase domain 2 (PHD2) and factor inhibiting HIF (FIH). J. Inorg. Biochem. 2012; 113:25–30. [PubMed: 22687491]

23. Chowdhury R, McDonough Ma, Mecinović J, Loenarz C, Flashman E, Hewitson KS, Domene C, Schofield CJ. Structural basis for binding of hypoxia-inducible factor to the oxygen-sensing prolyl hydroxylases. Structure. 2009; 17:981–989. [PubMed: 19604478]

24. Koivunen P, Hirsilä M, Kivirikko KI, Myllyharju J. The length of peptide substrates has a marked effect on hydroxylation by the hypoxia-inducible factor prolyl 4-hydroxylases. J. Biol. Chem. 2006; 281:28712–28720. [PubMed: 16885164]

25. Flashman E, Bagg EaL, Chowdhury R, Mecinović J, Loenarz C, McDonough Ma, Hewitson KS, Schofield CJ. Kinetic rationale for selectivity toward N- and C-terminal oxygen-dependent degradation domain substrates mediated by a loop region of hypoxia-inducible factor prolyl hydroxylases. J. Biol. Chem. 2008; 283:3808–3815. [PubMed: 18063574]

26. Quinn DM, Sutton LD. Theoretical Basis and Mechanistic Utility of Solvent Isotope Effects. Enzyme Mechanism from Isotope Effects. 1991:73–126.

27. Muthukumaran RB, Grzyska PK, Hausinger RP, McCracken J. Probing the iron-substrate orientation for taurine/alpha-ketoglutarate dioxygenase using deuterium electron spin echo envelope modulation spectroscopy. Biochemistry. 2007; 46:5951–5959. [PubMed: 17469855]

28. Ehrismann D, Flashman E, Genn DN, Mathioudakis N, Hewitson KS, Ratcliffe PJ, Schofield CJ. Studies on the activity of the hypoxia-inducible-factor hydroxylases using an oxygen consumption assay. Biochem. J. 2007; 401:227–234. [PubMed: 16952279]

29. Hirsilä M, Koivunen P, Günzler V, Kivirikko KI, Myllyharju J. Characterization of the human prolyl 4-hydroxylases that modify the hypoxia-inducible factor. J. Biol. Chem. 2003; 278:30772–30780. [PubMed: 12788921]

30. Aragonés J, Schneider M, Van Geyte K, Fraisl P, Dresselaers T, Mazzone M, Dirkx R, Zacchigna S, Lemieux H, Jeoung NH, Lambrechts D, Bishop T, Lafuste P, Diez-Juan A, Harten SK, Van Noten P, De Bock K, Willam C, Tjwa M, Grosfeld A, Navet R, Moons L, Vandendriessche T, Deroose C, Wijeyekoon B, Nuyts J, Jordan B, Silasi-Mansat R, Lupu F, Dewerchin M, Pugh C, Salmon P, Mortelmans L, Gallez B, Gorus F, Buyse J, Sluse F, Harris Ra, Gnaiger E, Hespel P, Van Hecke P, Schuit F, Van Veldhoven P, Ratcliffe P, Baes M, Maxwell P, Carmeliet P. Deficiency or inhibition of oxygen sensor Phd1 induces hypoxia tolerance by reprogramming basal metabolism. Nat. Genet. 2008; 40:170–180. [PubMed: 18176562]

31. Chen Y-H, Comeaux LM, Eyles SJ, Knapp MJ. Auto-hydroxylation of FIH-1: an Fe(ii), alpha-ketoglutarate-dependent human hypoxia sensor. Chem. Commun. (Camb). 2008:4768–4770. [PubMed: 18830487]
32. Ryle MJ, Koehntop KD, Liu A, Que L, Hausinger RP. Interconversion of two oxidized forms of taurine/alpha-ketoglutarate dioxygenase, a non-heme iron hydroxylase: evidence for bicarbonate binding. Proc. Natl. Acad. Sci. U. S. A. 2003; 100:3790–3795. [PubMed: 12642663]
33. Mantri M, Zhang Z, McDonough Ma, Schofield CJ. Autocatalysed oxidative modifications to 2-oxoglutarate dependent oxygenases. FEBS J. 2012; 279:1563–1575. [PubMed: 22251775]
34. Liu, a; Ho, RY.; Que, L.; Ryle, MJ.; Phinney, BS.; Hausinger, RP. Alternative reactivity of an alpha-ketoglutarate-dependent iron(II) oxygenase: enzyme self-hydroxylation. J. Am. Chem. Soc. 2001; 123:5126–5127. [PubMed: 11457355]
35. Fu A, Tang R, Hardie J, Farkas ME, Rotello VM. Promises and pitfalls of intracellular delivery of proteins. Bioconjug. Chem. 2014; 25:1602–1608. [PubMed: 25133522]
36. Ye S, Price JC, Barr EW, Green MT, Bollinger JM, Pennsyl V, Uni S, Park UV. Cryoreduction of the NO-Adduct of Taurine : r -Ketoglutarate Dioxygenase (TauD) Yields an Elusive {FeNO} 8 Species. J. Am. Chem. Soc. 2010; 132:4739–4751. [PubMed: 20218714]
37. Han AY, Lee AQ, Abu-Omar MM. EPR and UV-vis studies of the nitric oxide adducts of bacterial phenylalanine hydroxylase: effects of cofactor and substrate on the iron environment. Inorg. Chem. 2006; 45:4277–4283. [PubMed: 16676991]
38. Hausinger RP. FeII/alpha-ketoglutarate-dependent hydroxylases and related enzymes. Crit. Rev. Biochem. Mol. Biol. 2004; 39:21–68. [PubMed: 15121720]
39. Ray M, Golombek AP, Hendrich MP, Yap GPa, Liable-Sands LM, Rheingold AL, Borovik aS. Structure and Magnetic Properties of Trigonal Bipyramidal Iron Nitrosyl Complexes. Inorg. Chem. 1999; 38:3110–3115.
40. Saban E, Flagg SC, Knapp MJ. Uncoupled O2-activation in the human HIF-asparaginyl hydroxylase, FIH, does not produce reactive oxygen species. J. Inorg. Biochem. 2011; 105:630–636. [PubMed: 21443853]
41. Kahnert A, Kertesz MA. Characterization of a sulfur-regulated oxygenative alkylsulfatase from Pseudomonas putida S-313. J. Biol. Chem. 2000; 275:31661–31667. [PubMed: 10913158]

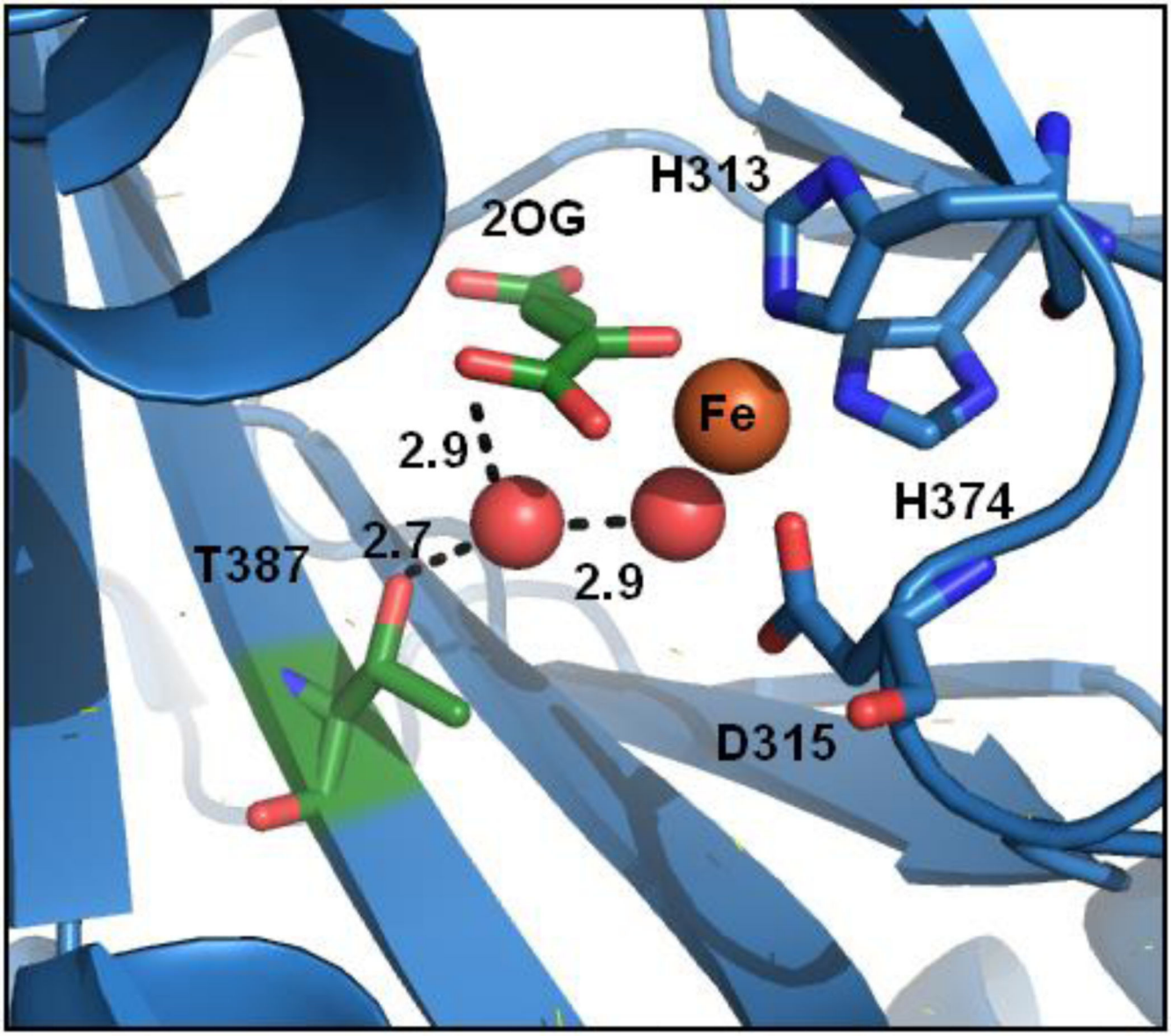

Figure 1.
PHD2 active site (PDB ID: 3OUJ).[16] Waters (red sphere), distances (Å).

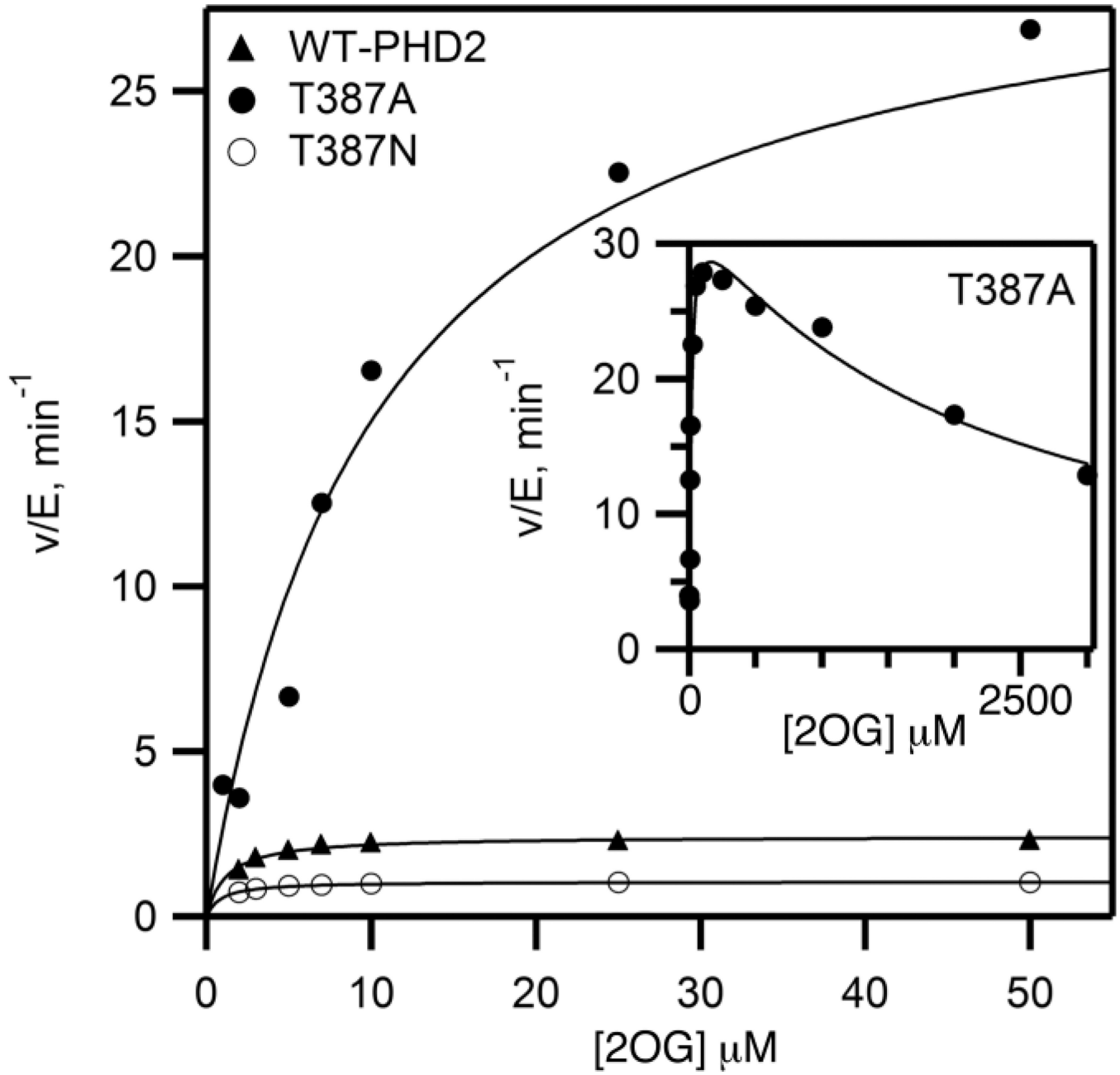

Figure 2.

Steady state kinetics for PHD2 variants with varied [2OG]. Reaction mixtures included $(NH_4)_2Fe(SO_4)_2$ (10 μM), ascorbic acid (1 mM), 2OG (1–3000 μM), and CODD (10 μM) in 50 mM HEPES pH 7.00, 37.0 °C, ambient $[O_2]$ (217 μM).

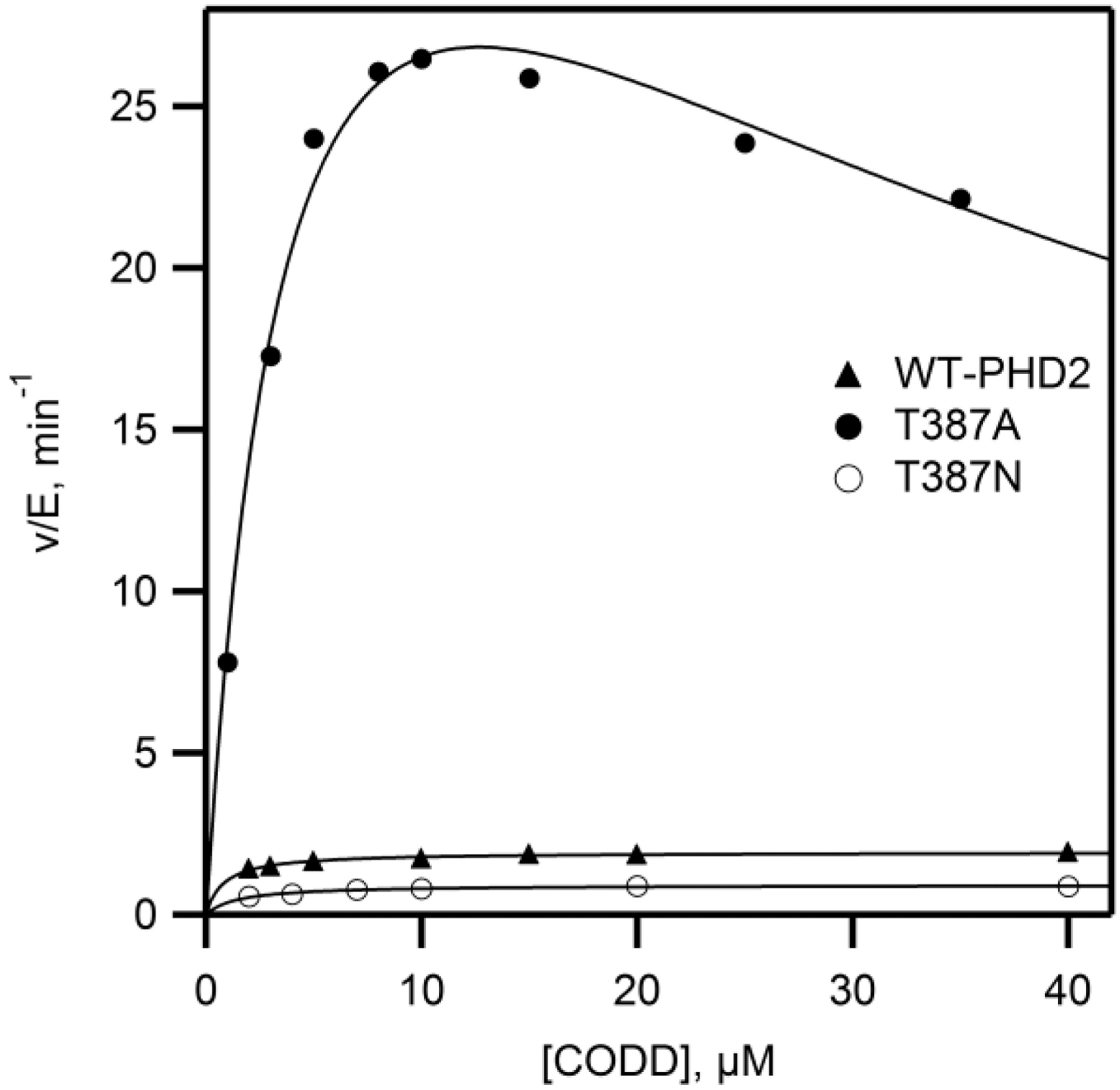

Figure 3.

Steady state kinetics data with varied [CODD]. Reactions included $(NH_4)_2Fe(SO_4)_2$ (10 μM), ascorbic acid (1 mM), 2OG (100 μM), and CODD (2–40 μM) in 50 mM HEPES pH 7.00, 37.0 °C, ambient $[O_2]$(217 μM).

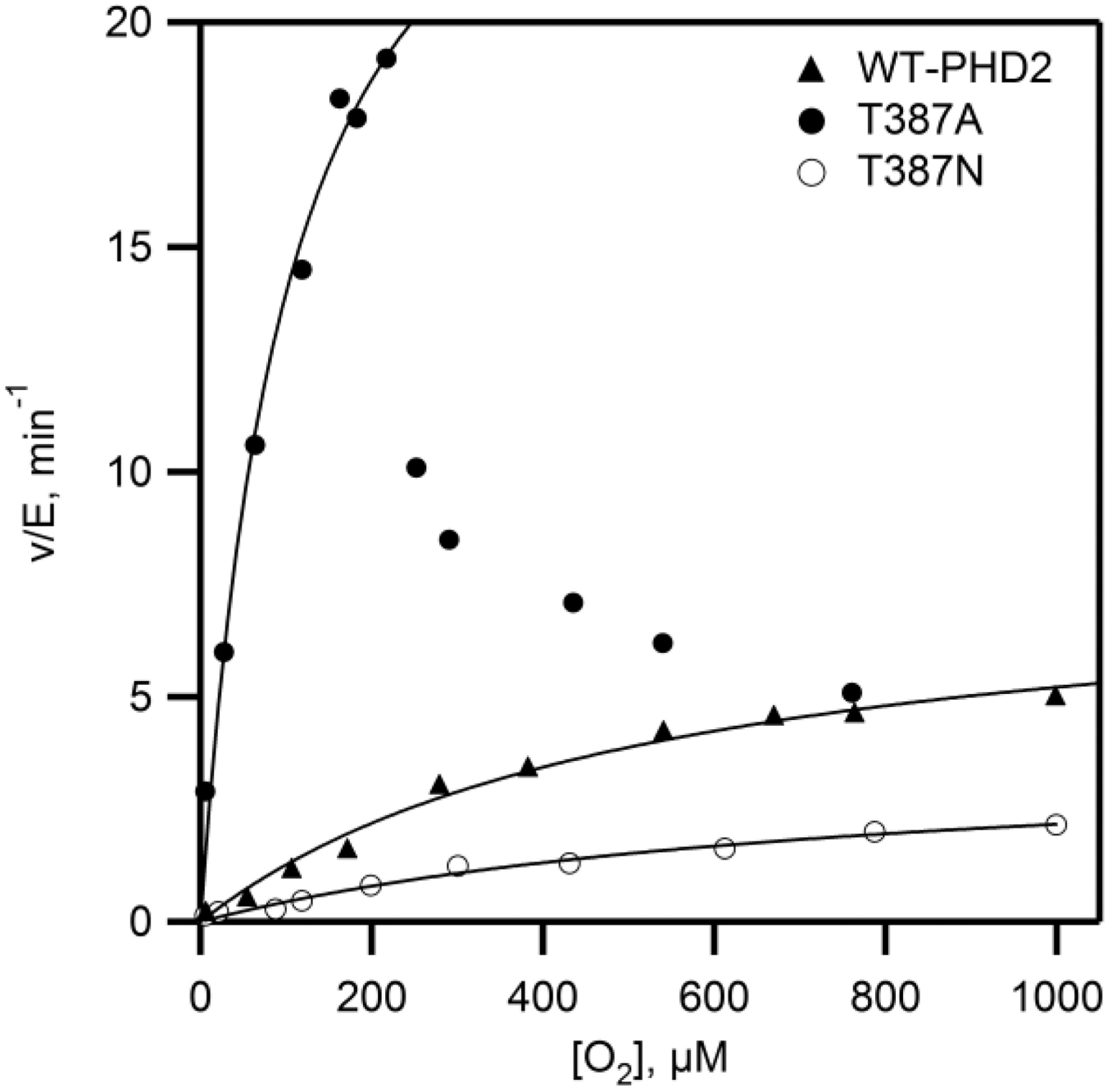

Figure 4.

Steady state kinetics as a function of varied $[O_2]$. Reaction mixtures included $(NH_4)_2Fe(SO_4)_2$ (10 μM), 2OG (100 μM), CODD (10 μM), and ascorbic acid (1 mM) in 50 mM HEPES pH 7.00. (open circles) WT-PHD2, (closed circles) $Thr^{387} \rightarrow Asn$, (triangles) $Thr^{387} \rightarrow Ala$.

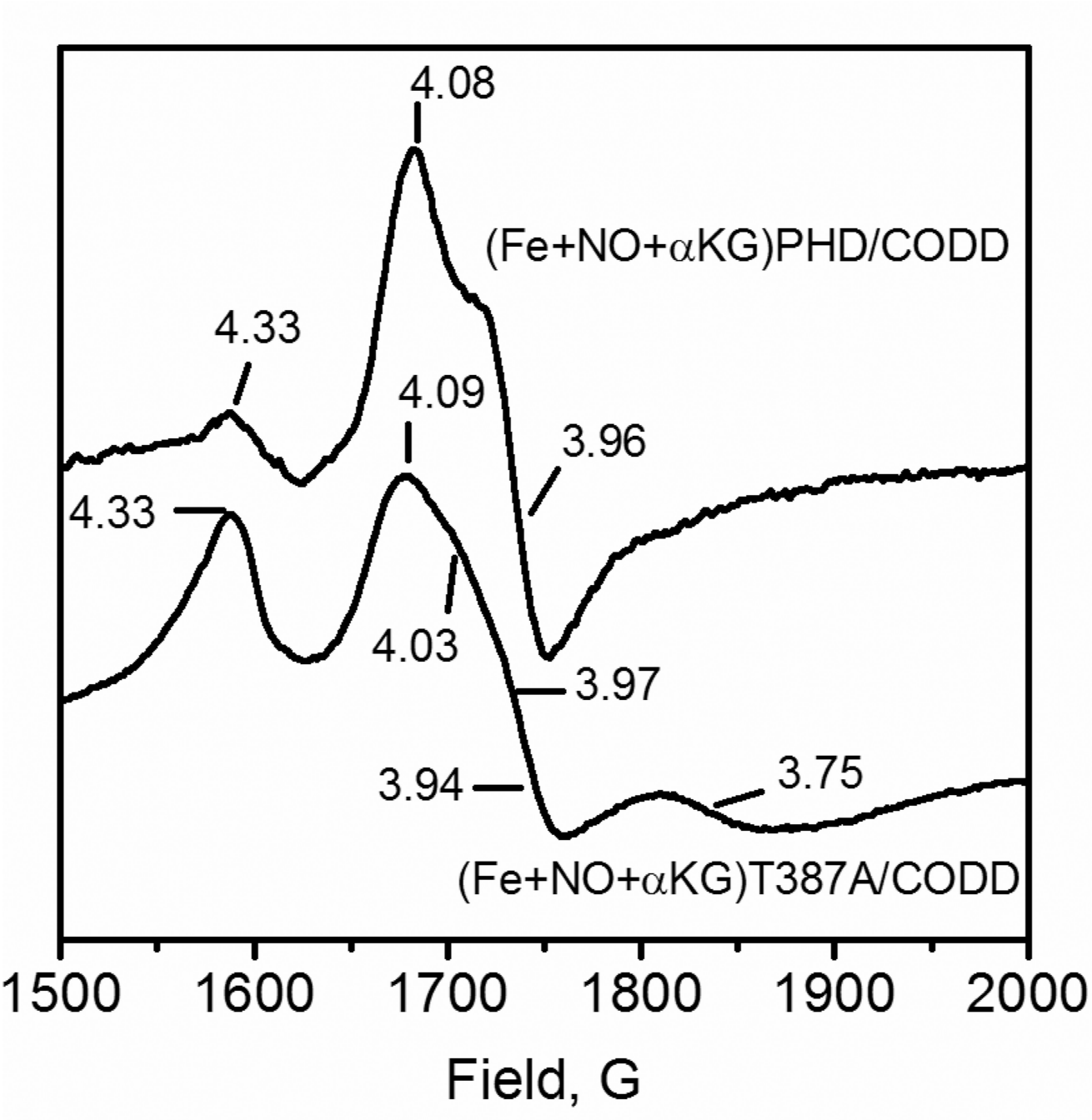

Figure 5.

X-band EPR of (Fe^{2+}+NO+2OG)PHD2/CODD. PHD2 (100 μM), CODD (100 μM), $(NH_4)_2FeSO_4$, (100 μM), 2OG (500 μM), and DEANO (500 μM) in 50 mM HEPES pH 7.00. 9.624 GHz frequency; 2.0 mW power; 10 G, 100 GHz modulation, 4 K.

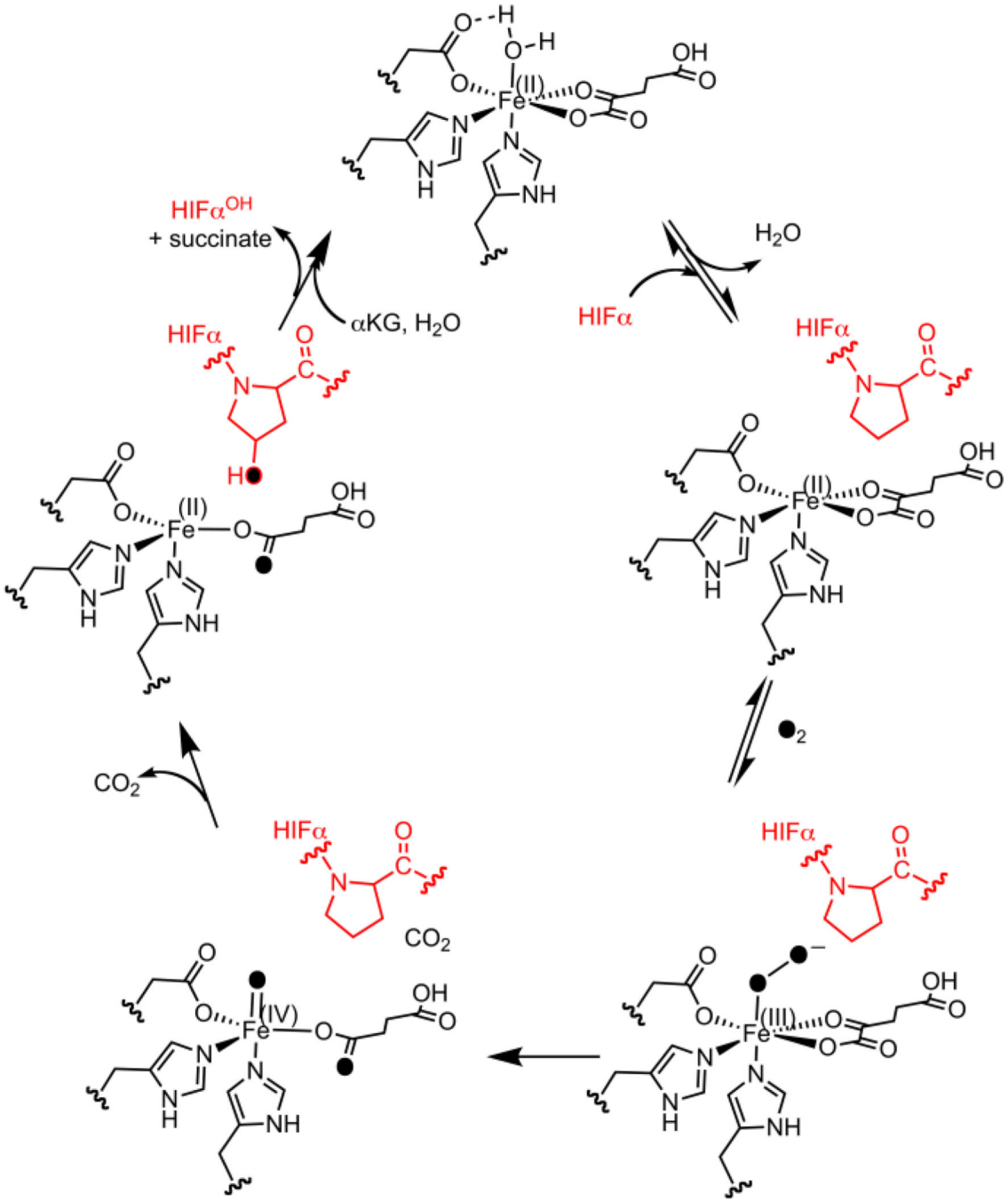

Scheme 1.
Consensus chemical mechanism for PHD2.

Table 1

Steady state kinetics of WT-PHD2 and variants with varied [2OG].[a]

Enzyme	k_{cat} min^{-1}	$k_{cat}/K_{M(2OG)}$ $\mu M^{-1}min^{-1}$	$K_{I(2OG)}$ μM	$K_{M(2OG)}$, μM	$K_{D(2OG)}$[b] μM
WT-PHD2	2.3 ± 0.1	2.7 ± 0.4	>2.6×10^4	0.9 ± 0.2	0.7 ± 0.2
Thr^{387}→Ala	32.9 ± 1.4	2.7 ± 0.3	2150 ± 340	12.0 ± 1.6	1.2 ± 0.2
Thr^{387}→Asn	1.0 ± 0.1	1.5 ± 0.2	>5×10^4	0.7 ± 0.1	0.6 ± 0.2

[a]. Reactions contained $(NH_4)_2Fe(SO_4)_2$ (10 μM), ascorbic acid (1 mM), 2OG (1–3000 μM), and CODD (10 μM) in 50 mM HEPES pH 7.00, 37°C, ambient $[O_2]$(217 μM).

[b]. Fluorescence titrations: PHD2 (1.1 μM), $MnSO_4$ (20 μM) in 50 mM HEPES pH 7.00 titrated with 2OG (500 μM).

Table 2

Steady state kinetic constants, k_{cat} and $k_{cat}/K_{M(CODD)}$ with varied [CODD].[a]

Enzyme	k_{cat}, min^{-1}	$k_{cat}/K_{M(CODD)}$, $\mu M^{-1}min^{-1}$	K_I, μM	K_M, μM
WT-PHD2	1.9 ± 0.1	2.4 ± 0.2	-	0.8 ± 0.1
Thr^{387}→Ala	44 ± 3	11 ± 1	38 ± 6	4.1 ± 0.7
Thr^{387}→Asn	0.9 ± 0.1	0.7 ± 0.1	-	1.4 ± 0.2

[a]. Reactions contained $(NH_4)_2Fe(SO_4)_2$ (10 μM), ascorbic acid (1 mM), 2OG (100 μM), and CODD (2 – 50 μM) in 50 mM HEPES pH 7.00, 37.0 °C, ambient $[O_2]$(217 μM).

Table 3

Steady state kinetic parameters using O_2 as the varied substrate.

Enzyme	k_{cat}, min^{-1}	k_{cat}/K_M, $\mu M^{-1}min^{-1}$	K_M, μM
WT-PHD2	8 ± 0.7	0.015 ± 0.001	530 ± 90
Thr^{387}→Ala	29 ± 3	0.3 ± 0.1	100 ± 20
Thr^{387}→Asn	3.8 ± 0.5	0.005 ± 0.001	760 ± 170

[Fe^{2+}] = 10 μM, [2OG] = 100 μM, [CODD] = 10 μM, 37.0°C, pH 7.00.